Degree-scale anomalies in the CMB: Localizing the first peak dip to a small patch of the north ecliptic sky

Amanda Yoho, Francesc Ferrer, and Glenn D. Starkman

Phys. Rev. D **83**, 083525 — Published 29 April 2011

DOI: 10.1103/PhysRevD.83.083525

Degree-scale anomalies in the CMB: localizing the first peak dip to a small patch of the north ecliptic sky

Amanda Yoho,[1] Francesc Ferrer,[2] and Glenn D. Starkman[3]

[1] *CERCA, Department of Physics, Case Western Reserve University, 10900 Euclid Avenue, Cleveland, OH 44106-7079, USA.*
[2] *Physics Department and McDonnell Center for the Space Sciences, Washington University, St Louis, MO 63130, USA*
[3] *CERCA/ISO, Department of Physics, Case Western Reserve University, 10900 Euclid Avenue, Cleveland, OH 44106-7079, USA.*

Noticeable deviations from the prediction of the fiducial LCDM cosmology are found in the angular power spectrum of the CMB. Besides large-angle anomalies, the WMAP 1^{st} year data revealed a dip in the power spectrum at $l \sim 200$, which seemed to disappear in the 3^{rd} year and subsequent angular power spectra. Using the WMAP single 1^{st}, 3^{rd}, and 5^{th} year data as well as the total 5 year coadded data, we study the intensity and spatial distribution of this feature in order to unveil its origin and its implications for the cosmological parameters. We show that in the 5-year coadded WMAP data release there is a suppression of the first Doppler peak in a region near the north ecliptic pole at a significance level between 99% and 96% depending on the weighting scheme that is considered.

PACS number: 98.80.-k

I. INTRODUCTION

The dynamics of both individual galaxies and clusters of galaxies, the Hubble diagram for distant Type Ia supernovae and the pattern of temperature anisotropies in the Cosmic Microwave Background (CMB) broadly support the standard flat Λ-dominated cosmological model with a nearly scale-invariant spectrum of adiabatic Gaussian primordial fluctuations, such as might be generated at the end of an inflationary epoch, as an accurate description of our universe.

In particular, this simple model provides an acceptable fit to the Wilkinson Microwave Anisotropy Probe (WMAP) observations of the CMB temperature anisotropies. The pattern of acoustic peaks and troughs predicted by the model to be imprinted on the angular power spectrum by the primordial fluctuations in the inflationary field and its subsequent evolution has been detected and characterized to good precision [1–3]. A global fit to the data has enabled cosmologists to determine the handful of parameters of the inflationary ΛCDM model, which does a remarkably good job at describing the spectrum.

The WMAP data, however, also exhibits unexpected anomalies that have sparked considerable attention [4, 5]. These include excesses or deficiencies of power in at least three bins – $\ell \sim 22$, 44 and 200 – violations of statistical isotropy at $\ell < 6$ [6–8], and a severe lack of large angle correlations requiring the low-ℓ C_ℓ to not be independent [2, 19]. Hemispheric asymmetries in the temperature power spectrum extending over a wide range of angular scales as well as hemispheric dependent non-gaussian signatures were reported in [9–12], and a non-Gaussian cold spot in the southern galactic hemisphere was found using wavelet transforms [14, 15]. Evidence for primordial non-Gaussianity of the local type in the temperature spectrum in the third year data has been claimed in [16] (However, it does not seem to be present when later data are included in the analysis [17, 18]).

If these anomalies are of primordial origin, rather than caused by unaccounted foreground or secondary effects, there could be profound implications for our understanding of the early Universe. For example, while the simplest single field inflationary scenarios predict negligible deviations from Gaussianity, larger deviations can be accommodated in extended particle physics models [21]. The lack of power in some low-ℓ multipoles, though not the multipole alignments and not the lack of large-angle correlations, could be explained by the presence of anticorrelated isocurvature perturbations such as those expected in the curvaton model [22, 23]. Topological defects could be at the origin of the cold spot [24].

Most of these anomalies were first noted in the first year WMAP data release and persisted into the subsequent data releases [19, 20]. The dip in the first peak found in the first year WMAP data release is believed to be a notable exception – it is no longer present when the newly adopted noise weighting scheme is used to extract the best fit power spectrum. This anomaly in the first year angular power spectrum was, thus, attributed to a noise fluctuation [3].

Surprisingly, the dip in the power spectrum around $\ell \sim 200$ disappears when data from the *ecliptic* poles is not included in the analysis of the 1st year WMAP data regardless of the weighting scheme (see Fig. 7 in [1]). Archeops, the sole previous ground-based experiment that observed the region of the sky around the north ecliptic pole, showed a dip around the first peak. All other similar experiments showed no such dip and had access only to southern ecliptic regions [25]. This suggests that the differences might not simply be due to a noise fluctuation, but might rather reflect a real anomaly.

In this paper we take a closer look at the degree-scale CMB temperature anisotropies. We estimate the primordial power spectrum using data from different regions of the sky according to the two weighting schemes that have been used by the WMAP collaboration. Our findings show that there is a substantial suppression of the first Doppler peak in a region near the north ecliptic pole. This reduction in the temperature power spectrum around the first acoustic peak occurs regardless of the weighting scheme used, although the detailed shape (i.e. the dip like feature) is only present when the analysis follows the strategy used by WMAP in their first year release and might also depend on the particular binning used to present the data.

The rest of the paper is organized as follows. In section II, we review the method used for estimating the power spectrum, C_ℓ, from observations. Section III describes the datasets that we used, together with the processing steps taken to minimize the influence of non-cosmological foregrounds. In section IV we discuss the method used to determine the statistical significance of our analysis of the data. Next, in section V, before our conclusions, we present the results of our analysis and briefly comment on implications for the physics underlying the CMB.

II. ESTIMATION OF POWER SPECTRA

Two main approaches have been used to estimate the power spectrum from a CMB data map, including sources of errors and partial sky coverage, namely maximum-likelihood estimators and pseudo-C_ℓ (PCL) methods. The WMAP team used the latter strategy for the analysis of their first year data, but changed to a hybrid estimator when producing the third year results, in agreement with the discussion in [26]. The differences, however, concern only the lowest multipoles ($\ell \leq 30$), which are not the object of our study. Hence, we base our results on the pseudo-C_ℓ technique [27], which we now briefly review.

The usual decomposition of a sky map $\Delta T(\mathbf{n})$ in spherical harmonics can be generalised to the case of partial sky coverage by introducing a position-dependent weight, $W(\mathbf{n})$, which is set to zero in the regions of the sky that are to be excluded from the analysis:

$$\tilde{a}^i_{\ell m} = \Omega_p \sum_p \Delta T^i(p) W^i(p) Y^*_{\ell m}(p)\,. \tag{1}$$

Here the map has been discretized in pixels sub-tending a solid angle Ω_p, and the index i refers to the particular differential assembly (DA) under scrutiny (see [1] for details on the datasets).

Even though the pseudo-power spectrum, $\tilde{C}_\ell$, derived from weighted maps (1),

$$\tilde{C}_\ell = \frac{1}{2\ell+1} \sum_{m=-\ell}^{\ell} |\tilde{a}_{\ell m}|^2, \tag{2}$$

differs from the full-sky angular spectrum, $C^{\rm sky}_\ell$, their ensemble averages are related by a mode coupling matrix, $G_{\ell\ell'}$, which can be inverted to obtain an estimator of the power spectrum:

$$\left\langle C^{\rm sky}_\ell \right\rangle = C_\ell = \sum_{\ell'} G^{-1}_{\ell\ell'} \tilde{C}_{\ell'}. \tag{3}$$

The coupling matrix depends only on the geometry of the weight function, $W(\mathbf{n})$. An expression for $W(\mathbf{n})$ can be found in [27].

In a multichannel experiment like WMAP, the noise between two different DAs is assumed to be uncorrelated. With a straightforward generalization of Eq. (2) for the analysis of two DA maps at a time,

$$\tilde{C}_\ell = \frac{1}{2\ell+1} \sum_{m=-\ell}^{\ell} \tilde{a}^i_{\ell m} \tilde{a}^{j*}_{\ell m}, \tag{4}$$

we obtain an estimate of the true power spectrum that is not biased by noise.

The weight function, $W(\mathbf{n})$, is zero where the foreground emission cannot be reliably eliminated. The main sources of non-cosmological origin (free-free, dust and synchrotron emission) are subtracted from each DA map by fitting templates and taking advantage of the different frequency dependence of each signal. The intensity of the foregrounds in the plane of the Galaxy, however, disallows a proper separation of the cosmological component in this region, which should be excluded from our analysis. We will set W to zero in the region specified by the KQ85 five year mask, an area of roughly 15% of the sky.

It is also advantageous to choose a different form of $W(\mathbf{n})$ in those regions where it is non-zero, depending on the multipole angular scale involved. Maximum-likelihood estimators, leading to smaller error bars, weight the data by the inverse covariance matrix, $C^{-1} = (S+N)^{-1}$, where S and N are the contributions from the signal and the instrument noise respectively. We can mimic this optimal sampling for the PCL estimator by using a unit uniform weight in the signal dominated, $C^{-1} \approx S^{-1}$, low ℓ regime. An inverse noise weight, $W^p \approx N^p_{obs}$, is more suitable for the noise dominated high multipoles [26]. In the first-year WMAP analysis, the two regimes were taken to be $\ell < 200$ and $\ell > 450$, while a transitional weighting interpolation was used for the intermediate multipoles [28]. For the third year analysis, the WMAP team used a sharp transition between the uniform weight and inverse noise weight at $\ell = 500$ (the transition was made at $\ell = 600$ for the seventh year analysis, although this does not affect our discussion). The fact that the dip-like feature in the first acoustic peak is not evident in the WMAP third year plot, lead the WMAP collaboration to conclude that it was largely due to the sharp weight transition at $\ell < 200$. We will see in the following that, in addition to this effect, the CMB power spectrum at these scales seems to vary markedly among different regions of the sky.

III. DATA SETS

The WMAP team obtained its best estimate power spectrum by optimally weighting all the possible pairings of Q, V and W DAs, although the Q band was dropped in the third year estimate, since it is the most prone to foreground and diffuse source contamination. Our aim here is not to obtain the best power spectrum estimate, but to study how it changes when looking at different parts of the sky or when using different weighting schemes. We thus obtain our power spectrum estimate by applying Eq. (3) to the foreground reduced V and W frequency band maps for the single first, third, and fifth year maps as well as the complete fifth year coadded map. We perform our analysis using the data processing method corresponding to each data release year as well as the applying the first and third year weighting schemes [1, 3] to all datasets.

Oddly enough, some of the anomalies found at large angular scales correlate with the ecliptic [7], and the WMAP team first year data gives a different angular power spectrum around $\ell \sim 200$ in the ecliptic plane than at the poles [1]. A random search in all directions could potentially reveal a more significant region, however when such an analysis was performed for the 1st year data the results also pointed to the ecliptic poles, as Eriksen, et al. found significantly low power in the northern hemisphere near the ecliptic pole for the range $\ell = 2 - 40$ [9]. We, thus, choose to examine two *a priori* selected 30 degree diameter spherical caps centered on the ecliptic poles. A later analysis (also on the first year data) that computed the directional dependence of the temperature power spectrum for an ℓ range that included the first peak was done in [13]. A comparison of those results with the results of our analysis is left for Section V.

Estimating the *real* power spectrum from observations of a limited region in the sky, introduces errors that increase as we shrink the patch. To minimize this effect we use *complementary masks*. For instance, *to check the influence of the northern ecliptic pole region, we just remove the cap around the pole and keep the rest of the sky.*

IV. ESTIMATION OF STATISTICAL SIGNIFICANCE

Masking a full sky map introduces correlations between the different multipoles that limit the precision of the estimated underlying power spectrum. Because our analysis of the data includes masking large regions near the ecliptic poles, we must determine whether our results are statistically significant or just a result of masking the map.

To do this, we generate 10^4 random realizations of the sky map from the best fit ΛCDM power spectrum. For each data release year and frequency band we wish to simulate we apply the corresponding beam transfer function, supplied by the WMAP team, to the extracted $a_{\ell m}$.

Next, we generate two identical maps of the sky and add uncorrelated noise to the pixels of each, given by the function

$$Noise \equiv \alpha \sigma_i(p), \tag{5}$$

where

$$\sigma_i(p) = \frac{\sigma_{0,i}}{\sqrt{N_{obs}(p)}} \tag{6}$$

is the noise for each pixel p in the ith frequency band map with $i =$ W or V. Here α is a randomly generated number with a Gaussian distribution, $\sigma_{0,i}$ the mean rms noise used to calculate the pixel noise for the ith band provided by [1], and $N_{obs}(p)$ is the number of observations recorded for pixel p that is taken from the corresponding data release year and frequency band WMAP data map we wish to simulate. This mimics the noise present in the V- and W-band data maps that, being independent, drops from the cross-correlation in Eq. (4).

Each map is then masked; first only the WMAP KQ85 mask is used, then the analysis is repeated with an additional region masked out (these regions include the north, south ecliptic poles and/or the ecliptic plane). We subtract the monopole and dipole, which are induced during masking, and calculate the cross-power spectrum using Eq. (4). Finally, we remove the window function and calculate the true $C_\ell s$ from the pseudo-$C_\ell s$ using Eq. (3).

We would like to quantify the relative difference between a map masked with only the KQ85 mask and the same map masked with KQ85 + some additional region. We have thus defined a peak statistic

$$S_{\rm peak} \equiv 2 \frac{\sum_{\ell=\ell_{min}}^{\ell_{max}} \left(C_\ell^{KQ85+add'l\ mask} - C_\ell^{KQ85} \right)}{\sum_{\ell=\ell_{min}}^{\ell_{max}} \left(C_\ell^{KQ85+add'l\ mask} + C_\ell^{KQ85} \right)}. \tag{7}$$

Here ℓ_{min} and ℓ_{max} are the extrema of a range of ℓ that covers the first peak of the power spectrum. The exact ℓ_{min}=200 and ℓ_{max}=250 values were chosen such that the value of $\ell_{max}(\ell_{max}+1)C_{\ell_{max}}$ and $\ell_{min}(\ell_{min}+1)C_{\ell_{min}}$ are 90% of the WMAP five year power spectrum peak value at its maximum.

V. RESULTS AND DISCUSSION

The observed power spectrum in the first year WMAP data for scales $\ell \sim 200$ was $\sim$10% smaller when using only the data from the ecliptic poles than what the best fit ΛCDM model would indicate. If this dip originated due to the lack of power entirely in a particular region in the sky, we can then estimate the diameter of the circular patch involved to be $\sim 30^\circ$.

As shown in Fig. 1, *the power around $\ell \sim 200$ increases if data in the region of the north ecliptic pole is*

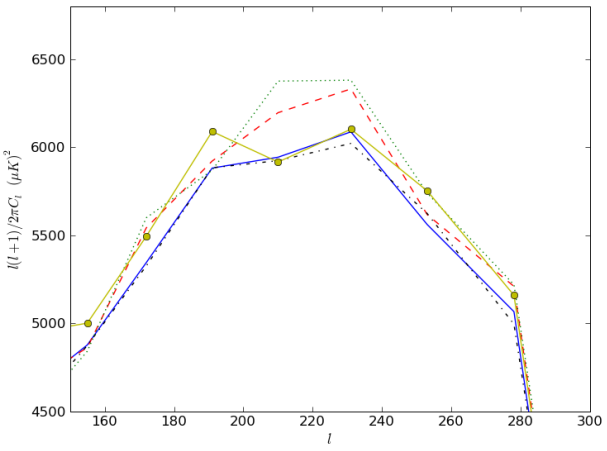

(a)First year data.

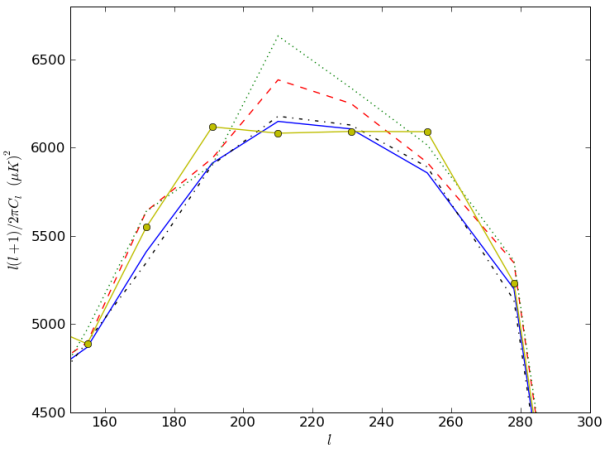

(b)Third year data.

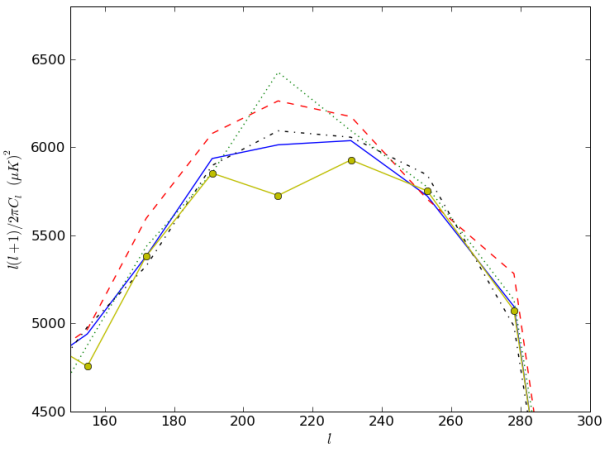

(c)Fifth year data.

FIG. 1. Power spectra for each data release year using the first year weighting schemes. We show the power spectra extracted from the full sky (blue solid), full sky without the north (red dashed) and south (black dot dashed) ecliptic caps, the ecliptic plane only (green dotted), and the ecliptic poles only (yellow circles). The galaxy is always masked out.

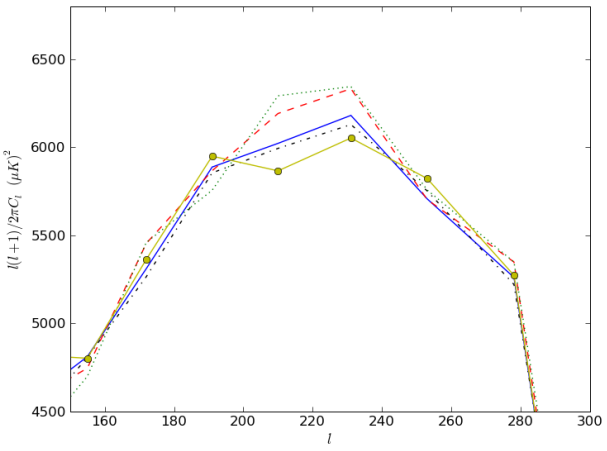

(a)First year data.

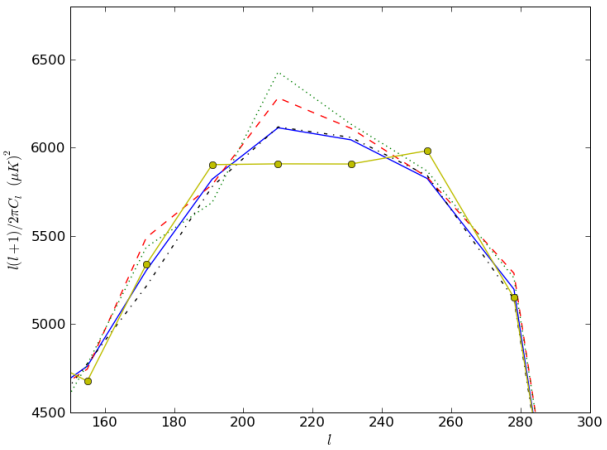

(b)Third year data.

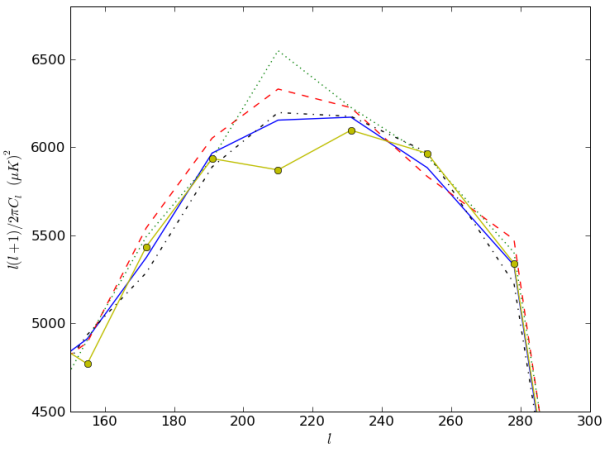

(c)Fifth year data.

FIG. 2. Power spectra for each data release year using the third year weighting schemes. We show the power spectra extracted from the full sky (blue solid), full sky without the north (red dashed) and south (black dot dashed) ecliptic caps, the ecliptic plane only (green dotted), and the ecliptic poles only (yellow circles). The galaxy is always masked out.

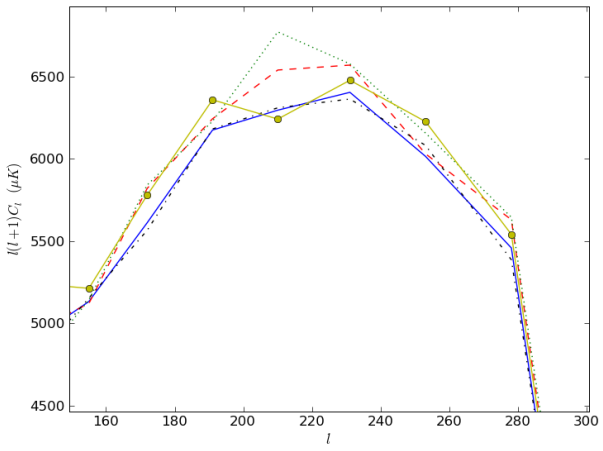

(a)First year weighting.

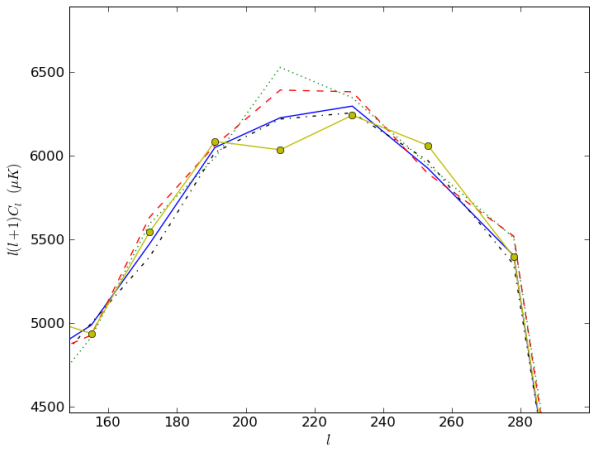

(b)Third year weighting.

FIG. 3. Power spectra for the full 5-year coadded data using both the first and third year weighting scheme. We show the power spectra extracted from the full sky (blue solid), full sky without the north (red dashed) and south (black dot dashed) ecliptic caps, the ecliptic plane only (green dotted), and the ecliptic poles only (yellow circles). The galaxy is always masked out.

masked out when estimating the spectrum. The blue solid line was obtained with the KQ85 mask only, and for the black dot dashed line we left out, in addition, the southern ecliptic pole. When leaving out the northern ecliptic pole (red dashed) or keeping just the ecliptic plane (green dotted) the value of $C_{\ell\sim200}$ is roughly 10% higher.

This effect is seen *for all WMAP data analyzed here regardless of the chosen weighting scheme* as shown in Fig. 2 for the third year weighting scheme analysis and, more importantly, in Fig. 3 where we have used the full 5 year coadded data. Although, the dip-like shape in the full sky minus the galaxy only appears when the first year data and weighting scheme is used. The 5 year coadded data is the most compelling part of the analysis, since there are far more observations per pixel and therefore less noise is in the resulting maps.

The significance of this effect can only be assessed with a detailed likelihood analysis. To this end, we have calculated the p-value for the peak statistic, given by Eq. 7, of each data release and weighting scheme. Figs. 4, 5, & 6 show the probability densities of peak statistic values found for the simulations masked with the KQ85 and north ecliptic+KQ85 masks for the first and third year weighting schemes respectively. The peak statistics and corresponding p-values (shown as percentages) for each data set are listed in Table I. These percentages are calculated by integrating under the curve in Figs. 4, 5, & 6 to the left of the specific value of the peak statistic found for the data. The significance is above $\sim$95% regardless of the data set and weighting scheme. Note that because the first year weighting scheme was developed for use with a noisy single year map, the values for the first, third, and fifth year data releases are probably most valid in the first column. With the cleaner, five-year coadded map the third year weighting scheme might possibly provide a better estimate.

The process of foreground cleaning was overhauled in the third year WMAP data release, and could account for the few percent drop in the significance value from the first to third year analysis. Still, the reduction in power due to northern ecliptic pole data is still significant (by about 2σ) in the later data releases.

As for possible systematic effects, it should be noted that the WMAP surveys the ecliptic plane more sparsely than the poles, and it has been suggested that beam ellipticity could bias the result. However, Wehus et al. [29] performed an extensive analysis of the effects of asymmetric beam patterns on the power spectrum, and found the change to be much smaller than what is shown in Figs. 1, 2 & 3 .

Hansen, et. al [13] performed an analysis on the first year WMAP data by varying the location of 9.5° and 19° disks around the sky and computing the power spectrum. They found that 3 disks resulted in a 2σ result, however this happened in 10% of their simulations which lead them to conclude that the effect was not significant. One important difference between the Hansen, et. al analysis and our own is that they used only the map data from inside the disk and consequently had use large ℓ bins to reconstruct the power spectrum. Our method, which uses complementary masks – analysis is on the data outside of the disc rather than inside – allows us to use a much smaller range of ℓ for each bin. Therefore, we are able to resolve the first peak in the power spectrum with a higher degree of accuracy (we have 6 points for $150 < \ell < 250$ whereas they have 2). We believe this could account for the difference in the determined significance of this effect.

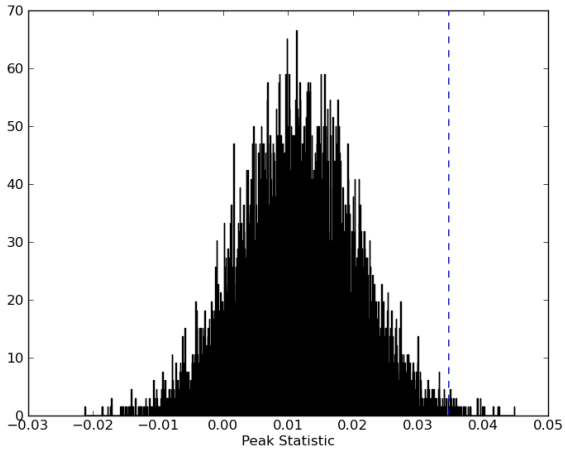

(a)

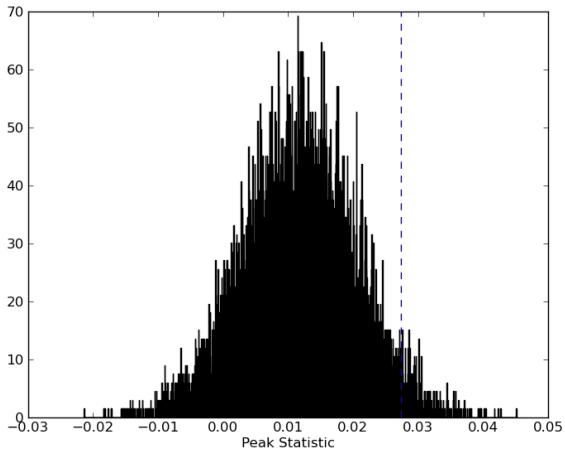

(b)

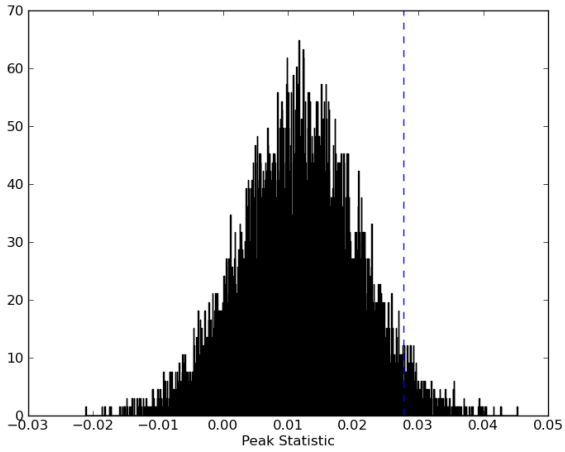

(c)

FIG. 4. Probability density of the peak statistics calculataed using first 4(a), third 4(b), and fifth 4(c) year simulated data for the first year weighting scheme. The y-axis shows the normalized number of Monte Carlo skies that have each particular value of S and the dashed blue line marks the peak statistic value calculated from the corresponding data release.

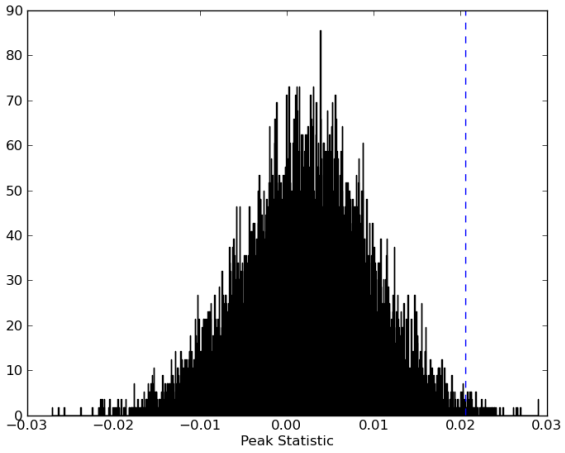

(a)

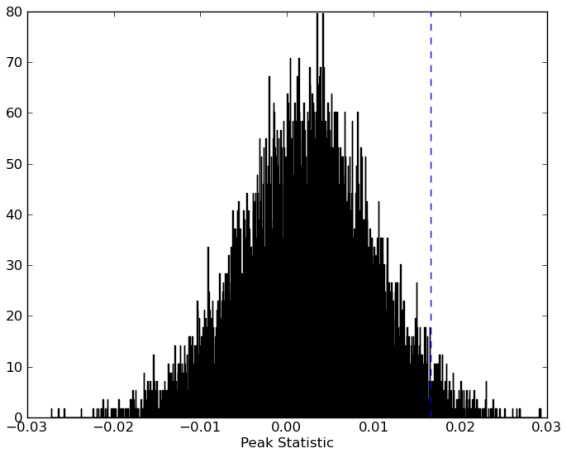

(b)

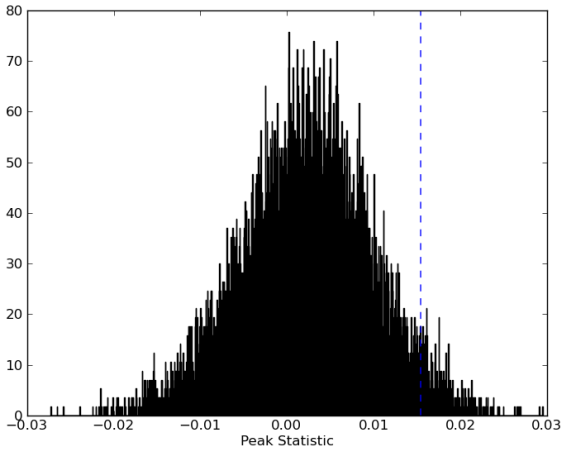

(c)

FIG. 5. Probability density of the peak statistics calculataed using first 5(a), third 5(b), and fifth 5(c) year simulated data for the third year weighting scheme. The y-axis shows the normalized number of Monte Carlo skies that have each particular value of S and the dashed blue line marks the peak statistic value calculated from the corresponding data release.

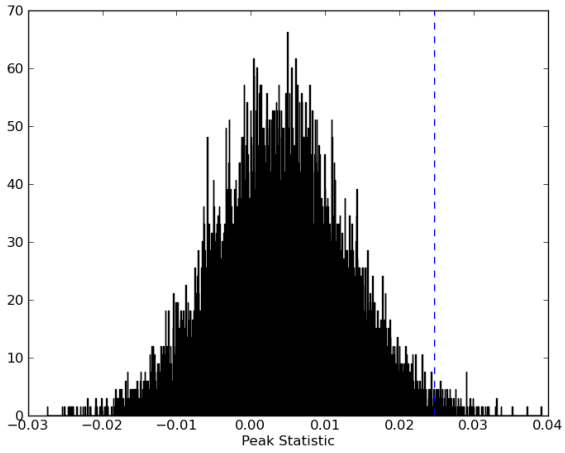

(a)First year weighting

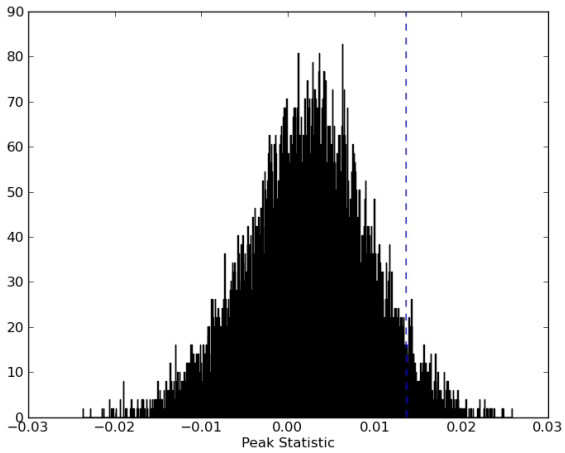

(b)Third year weighting

FIG. 6. Probability density of the peak statistics calculated using the five year coadded simulated data with the first 6(a), third 6(b) year weighting schemes. The y-axis shows the normalized number of Monte Carlo skies that have each particular value of S and the dashed blue line marks the peak statistic value calculated from the corresponding data release.

TABLE I. The first columns under the weight scheme headings list the peak statistic calculated for each data release. The second columns list the corresponding significance.

	1st year weighting		3rd year weighting	
1-year	.0347	99.57%	.0206	99.42%
3-year	.0274	96.70%	.0166	97.51%
5-year	.0278	96.94%	.0154	96.35%
5-year coadded	.0247	98.89%	.0136	95.61%

VI. CONCLUSION

In the first year WMAP TT power spectrum, the binned C_ℓ value at the first peak was significantly lower than the best-fit ΛCDM value [1]. This was widely referred to as the "dip in the first peak." In the third year data release the so-called dip disappeared. This was attributed to the use of an improved weighting scheme [3]. However, there was also shown to be a decrease in power at the first peak from the part of the sky near the ecliptic poles compared to the ecliptic plane in the first year data [1]. Indeed, using the improved (third year) weighting scheme, we have found that the ecliptic polar power at the first peak is significantly lower than the full-sky power in the first, third, fifth and coadded 5 year data releases. (We have not yet analyzed the seventh year data release, although we do not expect much difference.)

By separately masking out the north ecliptic polar region, the south ecliptic polar region and the ecliptic plane we have demonstrated that this difference can be ascribed to a large reduction in peak power in the north ecliptic polar region. We have shown that there is a significant increase in power when we mask out the north ecliptic pole for all weighting schemes and data releases. There is no such change in power when the south ecliptic pole is masked. Additionally, when using the third year weighting scheme there is still a sizeable reduction in power when only the data from the ecliptic poles is used compared to when the full sky is analyzed.

We have characterized the absence of power at the first doppler peak in the temperature power spectrum in the north ecliptic polar region using the peak statistic defined in Eq. 7. Using either the first or third year weighting scheme and across all data releases the significance is at least 95% based on 10^4 best-fit ΛCDM realizations and the analysis of one $V \times W$ cross-band power spectrum. The most trusted result should arguably be the significance of the coadded map with the third year weight scheme, as it provides analysis with the least noise and data processing method closest to what is currently used. Even when analyzing the most optimal data set for characterizing this effect, our result is still $\approx 2\sigma$ significant.

Indeed, the first peak may seem like a specific choice of range in ℓ to study – we would like to extend this analysis in the future to other "special" regions in ℓ-space, namely to the second and third doppler peaks. However current experiments are limited in their measurements around these peaks, so an accurate characterization of this effect is not possible. Future CMB experiments should provide better data for further analysis.

Archeops's observation of a dip in the first peak from measurements including the north ecliptic polar region of the sky, albeit at low statistical significance, suggests that this is not a WMAP systematic. Planck should therefore confirm the existence of a dip in the first peak power near the north ecliptic pole.

If these variations are of cosmological origin, they cannot be explained within the standard ΛCDM model, since

it predicts an isotropic and Gaussian spectrum. However, the association with the north ecliptic pole argues against a cosmological origin and in favor of Solar System physics. Possible signatures include a deviation in the CMB spectrum in this region of the sky and an associated anomaly in polarization maps.

ACKNOWLEDGMENTS

The authors were supported by a grant from the U.S. DOE to the Particle Astrophysics theory group at Case Western Reserve University and by NASA grant NNX07AG89G. F.F. was supported in part by the U.S. DOE under Contract No. DE-FG02-91ER40628 and the NSF under Grant No. PHY-0855580.

[1] G. Hinshaw *et al.* [WMAP Collaboration], Astrophys. J. Suppl. **148**, 135 (2003).

[2] D. N. Spergel *et al.* [WMAP Collaboration], Astrophys. J. Suppl. **148**, 175 (2003).

[3] G. Hinshaw *et al.* [WMAP Collaboration], Astrophys. J. Suppl. **170**, 288 (2007).

[4] C. L. Bennett *et al.*, arXiv:1001.4758 [astro-ph.CO].

[5] C. J. Copi, D. Huterer, D. J. Schwarz and G. D. Starkman, arXiv:1004.5602 [astro-ph.CO].

[6] A. de Oliveira-Costa, M. Tegmark, M. Zaldarriaga and A. Hamilton, Phys. Rev. D **69**, 063516 (2004).

[7] D. J. Schwarz, G. D. Starkman, D. Huterer and C. J. Copi, Phys. Rev. Lett. **93**, 221301 (2004).

[8] K. Land and J. Magueijo, Phys. Rev. Lett. **95**, 071301 (2005) [arXiv:astro-ph/0502237].

[9] H. K. Eriksen, F. K. Hansen, A. J. Banday, K. M. Gorski and P. B. Lilje, Astrophys. J. **605**, 14 (2004) [Erratum-ibid. **609**, 1198 (2004)].

[10] C. Räth, G.E. Morfill, G. Rossmanith, A.J. Banday, K.M. Gorski Phys. Rev. Lett. **102**, 131301 (2009) [arXiv:0810.3805 [astro-ph]].

[11] G. Rossmanith, C. Räth, A. J. Banday and G. Morfill, arXiv:0905.2854 [astro-ph.CO].

[12] F. K. Hansen, A. J. Banday, K. M. Gorski, H. K. Eriksen and P. B. Lilje, Astrophys. J. **704**, 1448 (2009) [arXiv:0812.3795 [astro-ph]].

[13] F. K. Hansen, A. J. Banday and K. M. Gorski, Mon. Not. Roy. Astron. Soc. **354**, 641 (2004) [arXiv:astro-ph/0404206].

[14] P. Vielva, E. Martinez-Gonzalez, R. B. Barreiro, J. L. Sanz and L. Cayon, Astrophys. J. **609**, 22 (2004) [arXiv:astro-ph/0310273].

[15] M. Cruz, E. Martinez-Gonzalez, P. Vielva and L. Cayon, Mon. Not. Roy. Astron. Soc. **356**, 29 (2005) [arXiv:astro-ph/0405341].

[16] A. P. S. Yadav and B. D. Wandelt, Phys. Rev. Lett. **100**, 181301 (2008) [arXiv:0712.1148 [astro-ph]].

[17] E. Komatsu *et al.* [WMAP Collaboration], Astrophys. J. Suppl. **180**, 330 (2009) [arXiv:0803.0547 [astro-ph]].

[18] K. M. Smith, L. Senatore and M. Zaldarriaga, JCAP **0909**, 006 (2009) [arXiv:0901.2572 [astro-ph]].

[19] C. Copi, D. Huterer, D. Schwarz and G. Starkman, Phys. Rev. D **75**, 023507 (2007).

[20] H. K. Eriksen, A. J. Banday, K. M. Gorski, F. K. Hansen and P. B. Lilje, Astrophys. J. **660**, L81 (2007).

[21] N. Bartolo, E. Komatsu, S. Matarrese and A. Riotto, Phys. Rept. **402**, 103 (2004) [arXiv:astro-ph/0406398].

[22] C. Gordon and A. Lewis, New Astron. Rev. **47**, 793 (2003).

[23] F. Ferrer, S. Rasanen and J. Valiviita, JCAP **0410**, 010 (2004) [arXiv:astro-ph/0407300].

[24] M. Cruz, N. Turok, P. Vielva, E. Martinez-Gonzalez and M. Hobson, Nature **318**, 1612 (2007) [arXiv:0710.5737 [astro-ph]].

[25] X. Wang, M. Tegmark, B. Jain and M. Zaldarriaga, Phys. Rev. D **68**, 123001 (2003) [arXiv:astro-ph/0212417].

[26] G. Efstathiou, Mon. Not. Roy. Astron. Soc. **349**, 603 (2004) [arXiv:astro-ph/0307515].

[27] E. Hivon, K. M. Gorski, C. B. Netterfield, B. P. Crill, S. Prunet and F. Hansen, Astrophys. J. **567**, 2 (2002) [arXiv:astro-ph/0105302].

[28] L. Verde *et al.* [WMAP Collaboration], Astrophys. J. Suppl. **148**, 195 (2003) [arXiv:astro-ph/0302218].

[29] I. K. Wehus, L. Ackerman, H. K. Eriksen and N. E. Groeneboom, Astrophys. J. **707**, 343 (2009) [arXiv:0904.3998 [astro-ph.CO]].